ARTICLE
TMR Modern Herbal Medicine 2023;6(4):20. https://doi.org/10.53388/MHM2023020

Exploring the mechanism of action of bei shashen-maidong in the treatment of non-small cell lung cancer based on network pharmacology and experimental validation

Yuan-Cai Liu[1#], Jia-Ying Yang[1#], Xia-Cheng Zhou[1], Xiang Qian[2], Zhuo Chen[2], Meng-Ying Sun[1], Yang-Bo Tong[1], Ai-Qin Zhang[2]*

[1]The Second Clinical Medical College, Zhejiang Chinese Medical University, Hangzhou 310053, China. [2]Department of Traditional Chinese Medicine, Zhejiang Provincial Cancer Hospital, Hangzhou 310005, China.

[#]These authors contributed equally to this work and are co-first authors for this paper.

***Corresponding to:** Ai-Qin Zhang, Department of Traditional Chinese Medicine, Zhejiang Provincial Cancer Hospital, No.1 Banshan East Road, Gongshu District, Hangzhou 310005, China. E-mail: zhanghaojianbb@163.com.

Author contributions

Liu YC, Yang JY and Qian X collected data. Liu YC and Chen Z conducted data analysis, Qian X and Chen Z purchased experimental materials, Liu YC, Sun MY , Tong YB and Zhou XC conducted experiments, Liu YC and Yang JY wrote this article, and Zhang AQ reviewed and edited it.

Competing interests

The authors declare no conflicts of interest.

Acknowledgments

This research was supported by "Zhejiang Province Chinese Medicine Science and Technology Program Key Projects" (No.2021ZZ008).

Peer review information

TMR Modern Herbal Medicine thanks all anonymous reviewers for their contribution to the peer review of this paper.

Abbreviations

NSCLC, non-small cell lung cancer; BSS, Beishashen; MD, Maidong; PPI, protein-protein interaction; TCMSP, Traditional Chinese Medicine Systems Pharmacology; TCM, traditional Chinese medicine.

Citation

Liu YC, Yang JY, Zhou XC, et al. Exploring the mechanism of action of bei shashen-maidong in the treatment of non-small cell lung cancer based on network pharmacology and experimental validation. *TMR Modern Herb Med*. 2023;6(4):20. doi: 10.53388/MHM2023020.

Executive editor: Ting Yu.

Received: 13 October 2023; **Accepted:** 30 November 2023; **Available online:** 01 December 2023.

Abstract

Beishashen (BSS) and Maidong (MD) are commonly used Medicine right for the treatment of non-small cell lung cancer (NSCLC), but their specific mechanism of action is not clear. In this study, network pharmacology and molecular docking techniques were used to investigate the molecular mechanisms of the therapeutic effects of BSS-MD on NSCLC and to experimentally validate some of the targets. The network pharmacology approach, including active ingredient and target screening, drug-compound-target network construction, protein-protein interaction (PPI) network, enrichment analysis, and molecular docking, was used to investigate the mechanism of action of Beisashen and Maitong on NSCLC. First, the active components of BSS-MD and their targets were predicted, of which 423 targets interacted with NSCLC targets. Then, network pharmacology showed that Stigmasterol, Quercetin, Alloisoimperatorin, Isoimperatorin, Beta-sitosterol were the core components of BSS-MD, and PLK1, HSP90AB1, and CDK1 were the key therapeutic targets. KEGG enrichment analysis indicated that the mechanism of action of BSS-MD in NSCLC treatment was related to the cell cycle. Then we further performed experimental validation. CCK-8 assay showed that BSS-MD inhibited LEWIS cell viability and promoted apoptosis in a dose-dependent manner. qPCR assay, immunofluorescence, and protein blotting experiments demonstrated that compared with the control group and the control group, the expression of PLK1, HSP90AB1, and CDK1 mRNAs and proteins were reduced in the treatment group ($P < 0.01$). Therefore, we conclude that BSS-MD can block cell cycle progression by inhibiting the expression of PLK1, CDK1, and HSP90AB1 mRNAs and proteins to inhibit lung cancer cell growth and promote apoptosis, and emphasize that BSS-MD are promising adjuvants for NSCLC treatment.

Keywords: non-small cell lung cancer; network pharmacology; beishashen; maidong; cell cycle; PLK1; CDK1; HSP90AB1

Introduction

Lung cancer is one of the most common malignant tumors in human beings and is the leading cause of cancer deaths. According to statistics, in 2020, about 816,000 people were diagnosed with lung cancer and 715,000 died in China [1]. Lung cancer is categorized into small cell lung cancer (SCLC) and non-small cell lung cancer (NSCLC), with NSCLC accounting for 80–85% of all lung cancers [2]. Lung cancer is mostly asymptomatic at first and is usually detected at an advanced stage, which makes its five-year survival rate about 23% [3]. Currently, the main treatment modalities for advanced NSCLC are chemotherapy, immunotherapy, and targeted therapy, but patients often terminate the treatment due to intolerance of their adverse effects. Therefore, it is urgent to find effective drugs with low side effects to treat NSCLC.

Chinese medicine can regulate the proliferation, apoptosis, adhesion, and migration of cancer cells, as well as inhibit tumor angiogenesis, change the host immune system, and inhibit tumor growth, Therefore, it has rich experience and unique advantages in treating lung cancer [4]. The main pathogenesis of lung cancer is the binding of Phlegm and blood Stasis (The main manifestations are the stinging pain of the local lump, or numbness and abandonment of the limbs, chest tightness and phlegm, or purple and dark blood clots in the sputum), Yin injury (A general term for all normal water fluids in the body, including the internal fluids of various viscera and body organs and their normal secretions), and Qi depletion (Qi is a subtle substance with strong vitality in the human body, and it is one of the basic substances that constitute the human body and maintain the life activities of the human body), and mixture of deficiency and reality. Therefore, for patients with advanced lung cancer, the treatment should mainly be nourishing Yin and moistening the lung. ShashenMaidong decoction originated from the famous doctor Wu Jutong's *Detailed Analysis of Epidemic Warm Diseases* in the Qing Dynasty, is a classic prescription for lung cancer treatment in traditional Chinese medicine, which has the efficacy of nourishing yin and moistening lungs, helping produce saliva and slake thirst, and it is commonly used to treat syndrome of yin deficiency due to lung heat (The course of the disease is long, the yin fluid is deficient, accompanied by fever), such as coughing, phlegm and blood, and dryness of the throat, etc. Modern pharmacology has found that ShashenMaidong decoction can increase the survival rate of lung cancer patients by inhibiting tumor growth, improving the tumor's anoxic environment, and enhancing the immune force of the organism [5]. BSS-MD is the primal medicine of ShashenMaidong decoction, Beishashen and Maidong are the principal medicine of ShashenMaidong decoction, both taste sweet and slightly bitter, and both enter the lung and stomach channels, the sweet and soft taste can nourish Yin, bitter cold can relieve heat, the two are compatible, strengthen the role of supplementing qi and nourishing Yin, clearing heat and promoting fluid. And according to modern pharmacological research, the active components of sasanqua polysaccharides and maitake polysaccharides can improve the immunity of the body [6]. However, the exact mechanism of BSS-MD in the treatment of NSCLC is less studied at present, especially at the molecular level.

Network pharmacology is a comprehensive discipline combining systems biology and cyberinformatics. In recent years, it has been widely used in new drug development [7]. According to systems biology, complex diseases such as cancer are not caused by mutations in a single target gene, but by mutations in multiple genes that lead to the disruption of the balance of the biological network system. Network pharmacology aims to study the balance of biological networks. It can analyze the effects of multi-component drugs on the human body at the system level, which helps us to find the therapeutic targets of drug active ingredients, improve drug efficacy, and reduce side effects [8]. Molecular docking is a computer simulation technique that models interactions between molecules and proteins at the atomic level, predicts the conformation of ligands and receptors, and calculates some parameters, such as affinities, which are used to evaluate the combination. The technique is accurate and low-cost and is currently used mainly for drug design and elucidation of biochemical pathways [9]. We combined network pharmacology, molecular docking, and experiments to analyze the active components, potential targets, and molecular mechanisms of BSS-MD for the treatment of NSCLC, and performed experimental validation.

Materials and methods

Based on network pharmacological analysis

Collection and screening of active chemicals in BSS-MD. The active ingredients of BSS were searched in the Traditional Chinese Medicine Systems Pharmacology (TCMSP, http://lsp.nwu.edu.cn/tcmsp.php) and screened based on oral bioavailability (OB) ≥ 30% and drug-likeness (DL) ≥ 0.8 [10]. Since the chemical composition of MD was not available in the TCMSP database, the BATMAN-TCM bioinformatics analysis tool for molecular mechanisms of traditional Chinese medicine (http://bionet.ncpsb.org/batman-tcm/) was utilized to retrieve the components of MD, and core cutoff ≥ 20 and adjusted *P*-values < 0.05 were used as screening criteria for the active ingredients and targets of action [11].

Prediction of potential drug targets and acquisition of NSCLC targets. The PubChem database (https://pubchem.ncbi.nlm.nih.gov) was searched for the SMILES of the obtained compounds and the SMILES were entered into the Swiss Target Prediction database (http://www.swisstargetprediction.ch) to predict the target and Uniprot number. The keyword "Non-small cell lung cancer" was entered into the GeneCards database(https://www.genecards.org/). All target genes were imported into the Uniprot database (https://www.uniprot.org/) for normalization, and Uniprot IDs were obtained. All duplicates were deleted after the aggregation of Uniprot IDs. And the Wayne diagram was plotted.

Building "drug-compound-target-disease" interaction networks and PPI networks. The active ingredients and targets were entered into Cytoscape 3.8.2 for visualization and analysis, and the common targets were uploaded into the STRING database to draw a PPI network diagram, with the confidence level set to greater than 0.9, and the results were imported into Cytoscape 3.8.2 for the screening of core targets.

Biological function and pathway enrichment analysis of core targets. The co-interacting targets were entered into the Metascape database (https://metascape.org/gp/index.html#/main/step1) and were subjected to GO bioprocess (BP), cellular component (CC), molecular function (MF) enrichment analysis, and KEGG pathway enrichment analysis, and the entries were filtered according to the P value from smallest to largest, respectively. Some entries were screened out respectively, and the GO enrichment analysis bar graph and KEGG pathway analysis bubble graph were drawn using the microbiology letter platform.

Molecular docking. To further determine the effects of the components on the NSCLC key targets, the key active ingredients of the TCM were screened based on the connectivity values, and the core targets were screened by the PPI network diagram. PyMOL and AutoDockTool 1.5.6 software were utilized to dock the key active ingredients with the core targets. The structure files of the key active ingredients (mol2 format) and the protein crystal structures of the core targets (pdb format) were obtained by downloading from PubChem and RSCB PDB databases, respectively.

Experimental verification

Materials. Animals: 20 male SD rats of SPF grade, 6 ~ 8 weeks old, body mass (250 ± 20) g, purchased from ICell Bioscience Inc, Shanghai. The rats have been examined by the Laboratory Animal Ethics Committee of Zhejiang Yingyang Pharmaceutical Research and Development Center, Ethics Approval No.: ZJET-20220314-01.

Cell line: Mouse Lewis cell line was purchased from ICell Bioscience Inc, Shanghai, Lot number iCell-m027.

Drugs, reagents and instruments. Drugs: 10g each of BSS and MD,

both purchased from Zhejiang Shouxiangu Pharmaceutical Co., Ltd.; Reagents: DME High Sugar Medium (gibco, batch number 2130493) , fetal bovine serum (sijiqing, batch number 21110705), Trypsin 0.25% (1 ×) Solution (TransGen Biotech, batch number Q30323), PBS phosphate buffer (pH 7.2–7.4) (TRANSGEN BIOTECH, batch number O21023), Cell Counting Kit-8 (CCK8 kit) (Beyotime Biotechnology, batch number 112921220216), RIPA lysate (Beyotime Biotechnology, batch number 090121211229), PMSF (Beyotime Biotechnology, batch number 20220212), SYBR Green qPCRkit (Yeasen Biotechnology (shanghai) Co., Ltd, batch number H0108041), reverse transcription kit (iangsu Cowin Biotech Co., Ltd., batch number 36320), protease inhibitor (iangsu Cowin Biotech Co., Ltd., batch number 50321), isopropanol (Mclean, batch number C12833389), BCA protein quantitatively kit (Solarbio, batch number 20220218), prepainted proteinmarker (Solarbio, batch number 326G022), wood spirit (Yongda, batch number 20220222), 30% acylamide (Biosharp, batch number H108KA8405), 1.5 M Tris PH 8.8 (Biosharp, batch number 22011373), 1.0 M Tris PH 6.8 Biosharp (Biosharp, batch number 21230507), BSA (BioFRoxx, batch number EZ7980B203), 10% APS (BBI Life Sciences, batch number H616BA1001）、PVDF membrane (millipore, batch number R1NB74016), SRC Antibody (Abcam, dilution ratio 1:1000, batch number GR5170787-24), β-actin Antibody (Affinity, dilution ratio 1:10000, batch number 12w2944), Instruments: low-temperature high-speed centrifuge, cell culture incubator, low-temperature high-speed centrifuge (Thermo); enzyme labeling instrument (MD); flow cytometer (Agilent); ordinary PCR (Eppendorf); mRNA quantifier (Thermo Scientific); real-time fluorescence quantitative PCR instrument (Roche, Switzerland); electrophoresis, electrophoresis tanks, transmembrane instrument (Tianneng); Chemiluminescence instrument (Qinxiang).

Methodologies. Preparation of aqueous decoction. 10 g each of BSS and MD were decocted twice according to the traditional method, and the liquid was merged. Preparation of drug-containing serum20 SD rats, male, were randomly divided into a control group and a drug administration group according to body weight. The rats in the drug administration group were gavaged twice a day in the morning and evening, and the administered dose (300 mg/kg) was determined according to the conversion method of the body surface area method of human rats for 5 consecutive days; the control group was given an equal amount of 0.9% NaCl solution, and after the last administration of 1 h, the rats were anesthetized, and the blood was taken from the heart, and it was left to stand for 2–3 h, the supernatant was aspirated, and it was centrifuged at 3000 r/min for 15 min, the supernatant was aspirated, and the same group of sera were mixed, and it was inactivated at 56 °C in a water bath for 30 min, and the sera were mixed with 0.22 μm pore filter membrane. Inactivate the serum at 56 ℃ for 30 min, filtered by 0.22 μm pore filter membrane, and stored at −80 ℃ for spare use.

Cell culture and grouping. Mouse LEWIS LC cells were cultured in fetal bovine serum, DME high glucose medium in a cell culture incubator, and the logarithmic growth phase cell suspension was taken for experiments. The cells were divided into 8 treatment groups (control group: cells not treated with drug-containing serum; blank serum control group: 10% blank serum-treated cells; drug-pair group: set drug-pair containing serum doses of 1%, 2%, 4%, 6%, 8%, and 10%), and were inoculated into 96-well plates after administration of the drug, and then incubated for the corresponding time, 10 μL of CCK-8 solution was added into each well, and incubated in the incubator.

CCK8 cell activity. The absorbance value at 450 nm (A value) was measured by enzyme labeling instrument, and the cell activity was calculated, cell activity = (A value of experimental group - blank zeroing A value)/(A value of control group - blank zeroing A value) × 100%. Each group of cells was measured in parallel with five replicate wells.

Apoptosis experiment. Take the logarithmic growth phase cells planted in 6 well cell culture plate, inoculation density of 1.2×10^6 cells per well, after 24 h culture. The cells were divided into 3 groups (A: control group: cells not treated with drug-containing serum; B: blank serum control group: cells treated with blank serum; C: drug-pair group: cells treated with 10% drug-containing serum) and collected after 48 h of treatment, washed twice with pre-cooled PBS, and adjusted the concentration of the cells to 1×10^6 cells/mL. 500 μL of binding buffer were added, and then centrifuged to discard the supernatant, and then 100 μL of binding buffer were added. After mixing, 5 μL of Annexin V-FITC and 10 μL of PI were added and mixed thoroughly; the reaction was performed at room temperature and protected from light for 15 min; finally, 400 μL of binding buffer was added, and the apoptosis rate was detected by flow cytometry within 1 h. The experiment was repeated three times. The experiment was repeated 3 times.

Real-time fluorescence quantitative PCR for the detection of PLK1, HSP90AB1, CDK1 mRNA expression in Lewis cells. The cells were cultured to 1×10^7 cells, 10% drug-containing serum was applied to treat the cellular interventions for 48 h. The cells at the bottom of the flasks were gently scraped off with a cell spatula, and total RNA was extracted using the Trizol method, and the concentration was calculated and then reverse transcription was performed using a reverse-transcription kit to reverse transcription. The primer sequences were shown in Table 1, and the reaction system was prepared according to the fluorescence quantitative PCR kit under the following conditions: 95 ℃, 10 min denaturation; 95 ℃, 15 s; 60 ℃, 60 s; 40 cycles. The data were quantified using the $2^{-\Delta\Delta CT}$ method to analyze the solubility curves and calculate the expression ratio of mRNA.

Western Blot assay to detect the expression of PLK1, HSP90AB1 and CDK1 proteins in Lewis cell. Weigh 100 mg of lung tissue, add 1 mL of cold Lysis Buffer lysis, homogenization, the cells discarded the supernatant, the cells were washed twice using PBS, the cells were harvested and centrifuged at 1000 rpm for 5 min, 600 μL of RIPA lysate was added (containing add 600 μL of RIPA lysate (containing PMSF and protease inhibitor), lysed on ice for 30 min, centrifuged at 12000 g for 5 min at 4 ℃, supernatant was taken, and the concentration was measured by BCA kit. Add Loading buffer (containing β-mercaptoethanol) (Loading buffer: β-mercaptoethanol = 50:3) (volume ratio of Loading buffer: sample = 1:4), boil water for 5 min denaturation, and then store at −20 ℃ for later use. 5% SDS-PAGE gel electrophoresis, 200 mA constant current for 120 minutes to turn the membrane, and 5% skimmed milk powder at room temperature. 5% skimmed milk powder was closed at room temperature for 1.5–2 h, primary antibody SRC (1:1000) was added, incubated at 4 ℃ overnight, washed with TBST for 10 min × 3 times, secondary antibody was incubated at room temperature for 2 h, washed with TBST for 10 min × 3 times, and developed by ECL chemiluminescence instrument.

Statistical treatment

All statistical data were analyzed using GraphPad Prism software V8.0. Differences between the two groups were measured by t-test, and comparisons between the groups were evaluated by one-way analysis of variance (ANOVA). The experimental data were expressed as mean ± SD. Statistical significance was defined as $P < 0.05$.

Table 1 Primer sequences

Gene	Forward primer	Reverse primer
Mouse PLK1	CCCGCTGGCGAAAGAAATTC	CATTTGGCGAAGCCTCCTTTA
Mouse HSP90AB1	AAACAAGGAGATTTTCCTCCGC	CCGTCAGGCTCTCATATCGAAT
Mouse CDK1	AGGTACTTACGGTGTGGTGTAT	CTCGCTTTCAAGTCTGATCTTCT
Mouse β-actin	ATGACCCAAGCCGAGAAGG	CGGCCAAGTCTTAGAGTTGTTG

TMR Modern Herbal Medicine 2023;6(4):20. https://doi.org/10.53388/MHM2023020

Results

Results of network pharmacology

Collection and screening of active chemical components in BSS-MD. 8 active components were obtained from BSS and 18 from MD, of which, Stigmasterol was the shared active component (Table 2).

Prediction of potential drug targets and acquisition of NSCLC targets. 444 BSS targets and 243 MD targets were obtained. After screening and standardization, 5580 NSCLC targets were obtained 423 common targets were obtained using an online Wayne diagram (Figure 1A).

Construction of "drug-compound-target" Interaction Networks and PPI Networks. A total of 450 nodes (2 drugs, 25 compounds, and 423 targets) and 811 edges were included in the "drug-compound-target" interaction network graph (Figure 2), and the top 10 key active ingredients and the top 5 core targets and some key targets were filtered according to the connectivity (Table 3). In the PPI network graph, there were 423 nodes and 1340 edges, and the topology analysis of the PPI network was performed by Cytoscape 3.8.2 (Figure 1B), and the top 23 core genes were filtered out based on the node's degree size (degree > 23) (Figure 1C).

Table 2 List of active chemical ingredients of BSS and MD

Chinese medicine name	molecule-name	Chinese medicine name	molecule-name
MaiDong/ BeiShaShen	Stigmasterol	MaiDong	Methyl Ophiopogonanone B
BeiShaShen	beta-sitosterol	MaiDong	Guanosine
BeiShaShen	quercetin	MaiDong	Ophiopogonin C
BeiShaShen	Alloisoimperatorin	MaiDong	Methyl Ophiopogonanone A
BeiShaShen	Ammidin	MaiDong	Ophiopogonanone C
BeiShaShen	isoimperatorin	MaiDong	Ophiopogonanone E
BeiShaShen	Bergaptin	MaiDong	N-Trans-Feruloyltyramine
BeiShaShen	Cnidilin	MaiDong	Ophiopogonin D
MaiDong	Ophiopogonone B	MaiDong	Ophiopogonin B
MaiDong	Ophiopogonin A	MaiDong	Orchinol
MaiDong	Uridine	MaiDong	Ophiopogon B
MaiDong	6-Aldehydo-Isoophipogonone B	MaiDong	Ophiopogon A
MaiDong	Ophiopogonanone A		

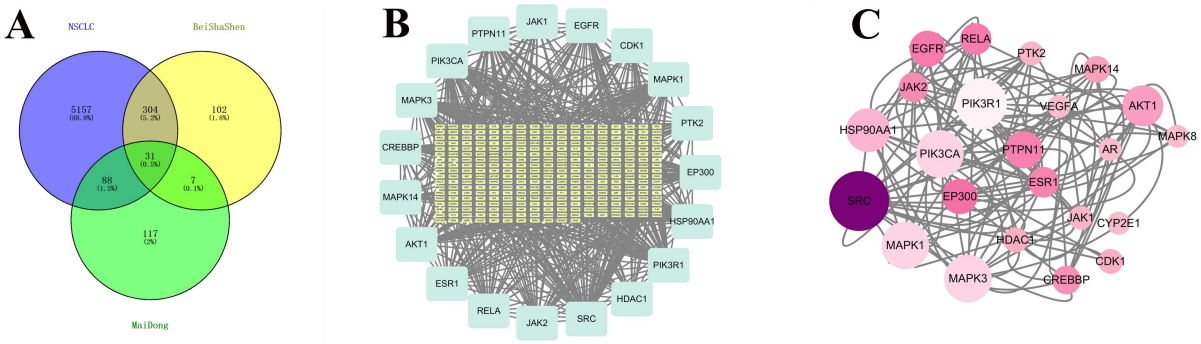

Figure 1 Potential therapeutic targets and PPI network map of BSS-MD for NSCLC. (A) Gene targets of BSS-MD and NSCLC. (B) Interaction network of targets for BSS-MD against NSCLC. (C) 23 core genes filtered based on degree size (degree > 23), the larger the node, the more important the protein is.

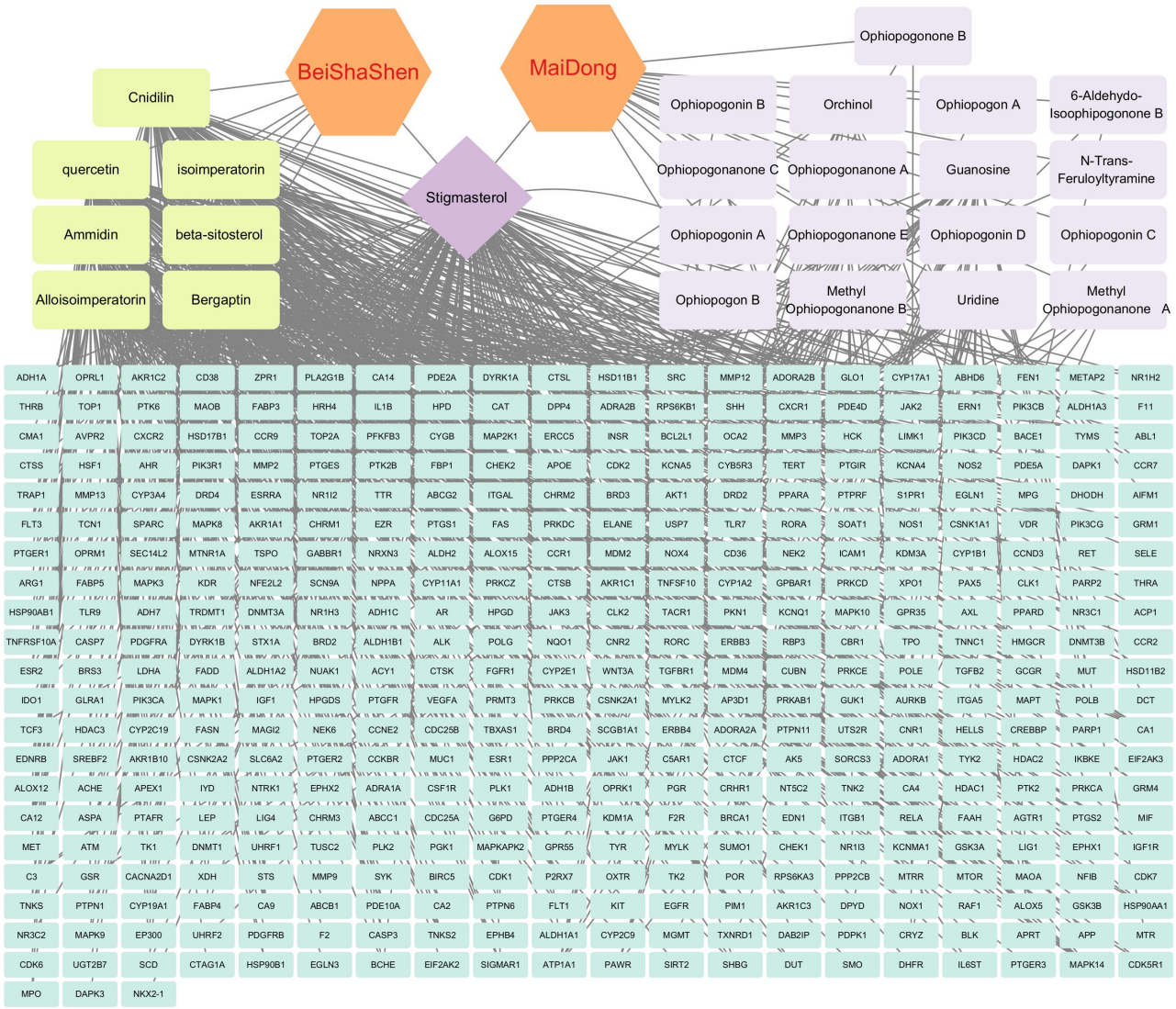

Figure 2 The drug-compound-target network. The orange nodes represent BSS and MD. The yellow color nodes represent the active ingredient of BSS. Mauve color nodes represent the active ingredient of MD. Dark purple color node represents the common active ingredient of BSS-MD. Azure blue nodes represent targets. Gray lines represent interconnections between nodes and nodes.

Table 3 Table of the top 10 key active ingredients and the top 5 core targets and some key targets

Name	Degree	Gene name	Degree
Stigmasterol	127	SRC	63
Quercetin	113	PIK3R1	54
Alloisoimperatorin	82	MAPK3	50
Isoimperatorin	76	PIK3CA	50
Beta-sitosterol	75	MAPK1	50
Bergaptin	75	CDK1	26
Cnidilin	75	CDC25A	12
Ammidin	65	HSP90AB1	12
Guanosine	29	PLK1	9
Uridine	20	CDC25B	8

GO enrichment analysis, KEGG pathway analysis. GO enrichment entries were obtained for a total of 227 GO entries, of which, BP: 201, CC: 1, and MF: 25; The top 10 GO entries enriched in BP, CC and MF are shown in (Figure 3A); A total of 167 KEGG pathways were obtained, among which the more highly enriched ones were PI3K-Akt signaling pathway, MAPK signaling pathway, cell cycle, etc., and the top 30 significantly enriched pathways are shown in (Figure 3B).

Molecular docking results. The binding energies of the key active ingredients to some of the core targets are shown in (Table 4), and most of the docking binding energies of these four active ingredients to the targets were below −2.5 kcal/mol, indicating good binding activity, which may be potential LC inhibitory targets. Some of the ligands and receptors were visualized and analyzed (Figure 4).

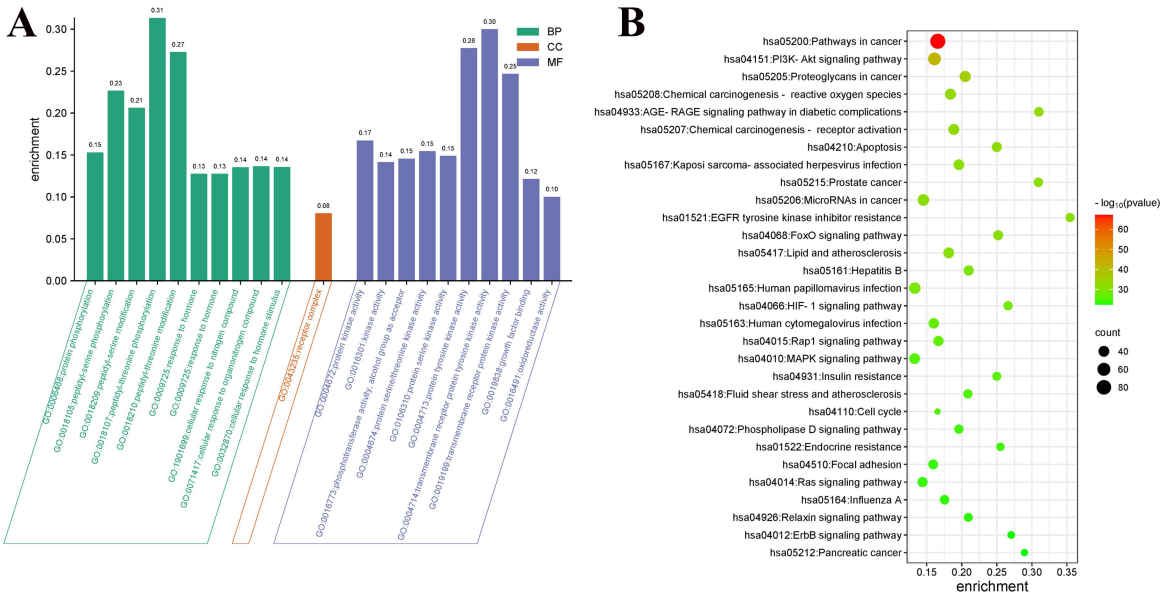

Figure 3 Biological process and pathway analyses from bioinformatics data. (A) GO functional analysis. (B) KEGG enrichment analysis. KEGG = Kyoto encyclopedia of genes and genomes.

Table 4 Molecular docking binding energy

Binding energy（−kcal/mol)	PLK1	HSP90AB1	CDK1
Stigmasterol	−5.81	−6.75	−6.75
Quercetin	−4.43	−3.46	−3.91
Alloisoimperatorin	−4.54	−5.09	−4.65
Isoimperatorin	−4.31	−5.36	−5.06

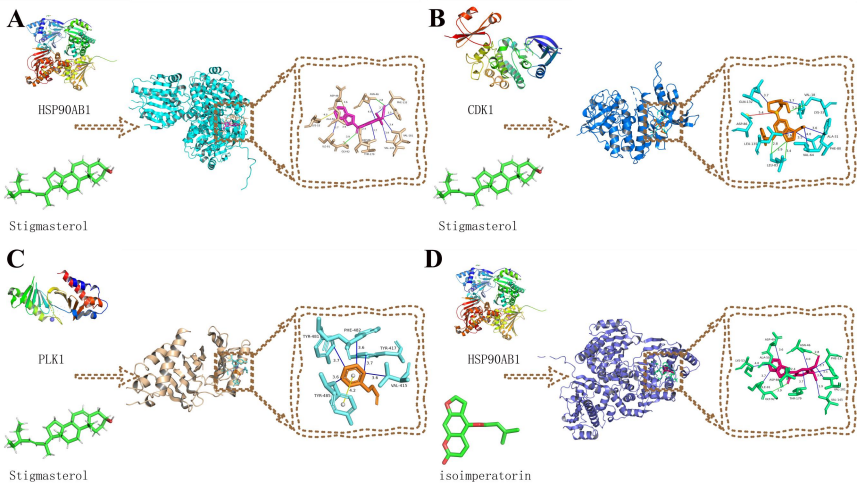

Figure 4 Molecular docking visualization diagram. (A) Molecular docking model of stigmasterol and HSP90AB1. (B) Molecular docking model of stigmasterol and CDK1, molecular docking model of isoimperatorin and HSP90AB1. (C) Molecular docking model of stigmasterol and PLK1.

Experimental results

Detection of cell viability. Compared with the blank serum group, the cell viability of LEWIS cells in the 8% and 10% drug-containing serum groups was significantly reduced after 24 h and 48 h ($P < 0.01$), and the cell viability of LEWIS cells in the 6% drug-containing serum group after 48 h ($P < 0.05$); the concentration of the drug and the cell viability were inversely proportional to each other (Figure. 5A).

Results of BSS-MD on apoptosis of LEWIS LC cells in each group. As shown by (Figure 5B/C), the apoptosis rate of LEWIS cells in the BSS-MD drug-paired group was significantly higher compared with the control group ($P < 0.01$).

Expression of PLK1, HSP90AB1, and CDK1 mRNA in LEWIS cells. From (Figure 6A), the expression levels of PLK1, HSP90AB1, CDK1 mRNA in LEWIS cells in the bitter almond-orchid drug pair group were significantly reduced compared to the control group ($P < 0.01$).

PLK1, HSP90AB1, CDK1 protein expression levels in LEWIS cells. As can be seen from Figure 6B/C, PLK1, HSP90AB1, CDK1 protein expression levels in LEWIS cells in the BSS-MD drug-pairing group were significantly reduced compared to the control group ($P < 0.01$).

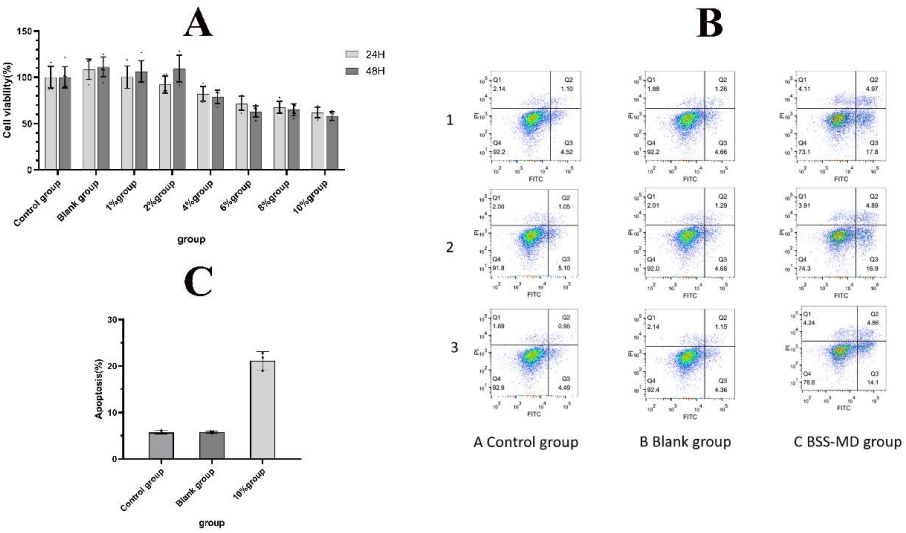

Figure 5 Cell viability and apoptosis graphs. (A) Cell viability. (Blank group = 10% blank serum control group; 1% group = 1% drug-containing serum group; 2% group = 2% drug-containing serum group; 4% group = 4% drug-containing serum group; 6% group = 6% drug-containing serum group; 8% group = 8% drug-containing serum group; 10% group = 10% drug-containing serum group). (B) Apoptosis status. (C) Apoptosis rate. (Blank group = 10% blank serum control group; BSS-MD group/10% group = 10% BSS-MD-containing serum treated cells).

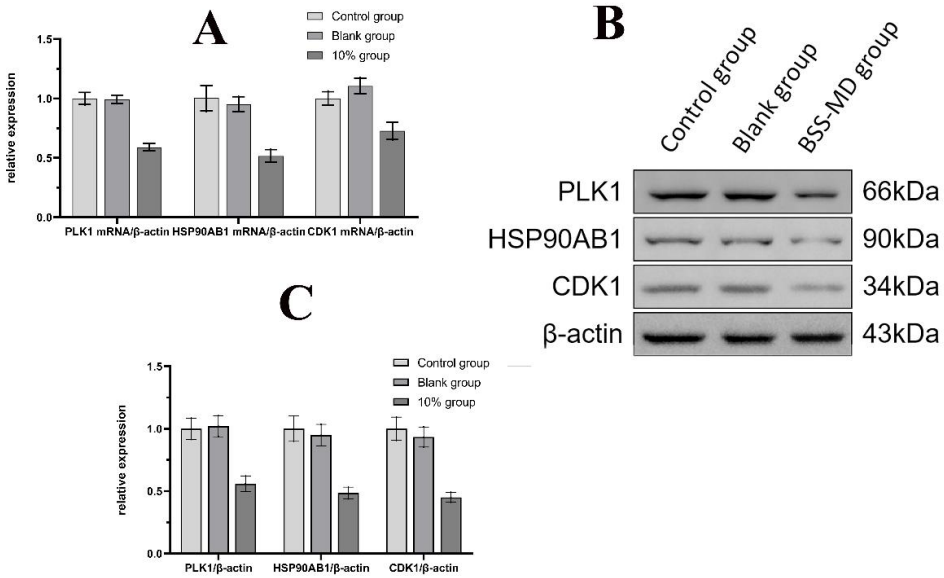

Figure 6 Expression of PLK1, HSP90AB1, CDK1 mRNA and protein in lung cancer LEWIS cells. (A) PLK1, HSP90AB1, CDK1 mRNA expression in LEWIS cells ($\bar{x} \pm s$, n = 3). (B) Strip chart of PLK1, HSP90AB1, CDK1 protein expression in LEWIS cells. (C) Histogram of PLK1, HSP90AB1, and CDK1 protein expression in LEWIS cells (Blank group = 10% blank serum control group; BSS-MD group/10% group = 10% BSS-MD-containing serum treated cells).

Discussion

Globally, lung cancer incidence and deaths are on the rise, with GLOBOCAN estimating 2.09 million new cases (11.6% of total cancer cases) and 1.76 million deaths (18.4% of total cancer deaths) in 2018, which is higher than the incidence reported in 2012 (1.8 million new cases and 1.6 million deaths), making it the most common and most deadly cancer in men, and the third most frequent and second most deadly cancer in women [12]. NSCLC accounts for 80–85% of all lung cancers and has a very high mortality rate, it has had a significant negative impact on people's lives [2]. However, effective drug therapy for NSCLC is still lacking. Many clinical studies have shown that anti-lung cancer treatment combined with TCM can reduce the side effects of radiotherapy, improve the therapeutic effect, and reduce complications. Meanwhile, TCM can prolong the life of lung cancer patients and improve their survival quality of life [13].

The most basic theory of TCM treatment for NSCLC is to regulate the imbalance by "strengthening the body" and "eliminating pathogenic factor" when the body's immunity is too weak and the tumor growth ability is too strong. "Strengthening the body" refers to enhancing the body's anti-cancer immunity, while "eliminating pathogenic factor" directly inhibits the growth, proliferation, invasion and migration of tumor cells [14]. According to Chinese medicine, Qi deficiency is the pathological basis of cancer [15]. Insufficient "Vital energy" makes it difficult to resist "Pathogenic factor", so that "Pathogenic factor" invades the body and accumulates, damaging the Yin fluid and eventually leading to the occurrence of lung cancer. ShashenMaidong decoction can strengthen the body by nourishing the body's "Vital energy" and "eliminate pathogenic factor" by resisting "Pathogenic factor", thus regulating the balance of the body and inhibiting tumor invasion. ShashenMaidong decoction is widely used in the treatment of lung cancer in clinical practice. Meiyan He et al. analyzed 104 patients with malignant lung cancer in primary lung cancer, and found that ShashenMaidong decoction could increase the PG-SGA score, KPS score, Chinese medicine evidence score, and serum albumin in patients with malignant lung cancer, and, at the same time, it could significantly reduce their tumor necrosis factor-α (TNF-α) and interleukin 6 (IL-6), which has clear therapeutic efficacy and important clinical value in the treatment of lung cancer cachexia, Yuying Zheng et al. found that ShashenMaidong decoction could inhibit tumor growth under intermittent hypoxic conditions by suppressing oxidative stress and inflammation through the establishment of Lewis lung cancer mouse model exposed to intermittent hypoxic conditions [6, 16]. BSS-MD are the primal medicine of ShashenMaidong decoction, which have the effects of replenish Qi, nourishing Yin, and clearing Heat, and several of the monomer compounds, such as Radix-Glehniace-Polysaccharide and Ophiopogon-Japonicus-Polysaccharide, can enhance the body's immunity and reduce cellular inflammatory factors, thus achieving anti-tumor effects [6, 17, 18]. Therefore, we used network pharmacology strategies and molecular docking to identify potential targets and mechanisms by which BSS, MD play a role in NSCLC and validated them with in vitro experiments.

First, we screened 26 active ingredients (Table 2), among which the main active ingredients are Stigmasterol, Quercetin, Alloisoimperatorin, Isoimperatorin, and Beta-sitosterol, which are the main chemical components that can act on multiple targets in the network together with other active ingredients. Stigmasterol triggers apoptosis in tumor cells by modulating the PI3K/Akt signaling pathway and mitochondrial reactive oxygen species production. It's antiproliferative activity is mainly dependent on its regulation of cell cycle proteins and cell cycle protein-dependent kinase (CDK) [19]. Quercetin decreased the expression of N-calmodulin, vimentin and ADAM9 by inhibiting the Snail-dependent Akt activation pathway, and increased the expression of E-calmodulin and MMP-related proteins significantly inhibiting lung cancer cell invasion and metastasis [20]. Some studies also found that Quercetin induced apoptosis in A549 cells by down-regulating IL-6/STAT-3 signaling and activating MEK-ERK [21]. Beta-sitosterol, as a potential natural drug, can be effective in preventing the development and growth of a variety of tumors. Rajavel et al. found that Beta-sitosterol up-regulated the levels of p53, pSer21–p460, and p72 in human lung cancer NCI-H15 cells, thereby mediating apoptosis and that Beta-sitosterol also induced ROS-dependent apoptosis in NSCLC cells through down-regulation of the thioredoxin (Trx)/thioredoxin reductase (TrxR1) signaling pathway [22, 23]. These findings suggest that these components may be important for the therapeutic efficacy of BSS-MD in the treatment of NSCLC and deserve further exploration.

Second, we retrieved 5580 candidate NSCLC targets from GeneCards database and predicted 444 BSS targets and 243 MD targets from SwissTarget Prediction database. We found 423 common targets between BSS-MD and NSCLC (Figure 1A), which are considered as potential targets for the treatment of NSCLC. The degree of association between these genes is shown in Figure 1B/C, and some of the core genes are shown in Table 3, including SRC, PIK3R1, MAPK3, PIK3CA, MAPK1, CDK1, CDC25A, HSP90AB1, PLK1, and CDC25B. These genes play important roles in the proliferation, migration, and apoptosis of NSCLC cells [24–26].

In order to investigate the mechanism of BSS-MD in the treatment of NSCLC, we performed GO analysis and KEGG enrichment analysis (Figure 3A/B). The GO results showed that the target genes were mainly enriched for biological functions such as protein phosphorylation, protein kinase activity, protein serine/threonine kinase activity, and tyrosine kinase activity of transmembrane receptor proteins. The results of KEGG enrichment analysis showed that BSS-MD were involved in a variety of signaling pathways in NSCLC treatment, mainly including PI3K-Akt signaling pathway, MAPK signaling pathway, Ras signaling pathway, Cell cycle and others. PI3K is a downstream effector that is activated in response to a variety of extracellular stimuli, and activated P13K phosphorylates AKT, which in turn promotes aggressive cancer behaviors such as cell proliferation, invasion, metastasis, and angiogenesis, and prevents programmed cell death by regulating several downstream effector; MAPK is a key signaling pathway that regulates a variety of cellular processes, including proliferation, differentiation, apoptosis, and stress responses [27, 28]. Previous studies have shown that inhibition of the PI3K-Akt and MAPK signaling pathways inhibits the proliferation, migration, and invasion of lung cancer cells [29]. Ras signaling is initiated and activated by G protein-coupled receptors (GPCRs) and receptor tyrosine kinases (RTKs). Ras promotes serine/threonine kinase (Raftransposition) to the plasma membrane, where it is turned on and phosphorylated by several protein kinases [30]. Raf moves through active Ras to the plasma membrane where it is activated and phosphorylated by several protein kinases. Active Raf phosphorylates and activates (mitogenic effector kinase) MEK1/2, which in turn phosphorylates (cytoplasmic signal-regulated kinase) ERK1/2, which then proceeds to act on mitogen-activated protein kinase (MAPK). In addition, Ras stimulates PI3K catalytic activity by interacting with the catalytic subunit p110α and mediates a closer interaction between PI110K and the plasma membrane. Thus, RTK can activate Ras, which in turn activates PI3K in a p110-dependent manner [31].

The cell cycle is the basic process of cell division, which is divided into four main phases: G1 phase (pre-DNA synthesis), S phase (DNA synthesis phase), G2 phase (late DNA synthesis), and M phase (mitosis), and it is mainly regulated by the cell cycle proteins, the cell cycle protein-dependent kinases (CDK), and the inhibitors of the cell cycle protein-dependent kinases [32]. With the induction of cell cycle proteins, each CDK is activated alternatively to drive the completion of the cell cycle in an orderly fashion [33]. CDK1 is the first member of the cell cycle protein-dependent kinase family and mediates multiple pathways to regulate cell division, autophagy and mitochondrial respiration, critical to mitotic progression [34–37]. For successful completion of mitosis, CDK1 activity is assisted by another important mitotic kinase, PLK1, They enhance each other's activity through multiple feedback loops [38, 39]. CDK1 activation is dependent on the accumulation of CDK2-mediated mitotic inducers

(e.g., PLK1), which at a threshold level induces switch-like activation and mitotic entry [40]. Cell cycle protein B is a G2 phase cell cycle protein that prepares cells to enter mitosis. It is synthesized in S phase and the protein is expressed in G2/M phase. In G2 phase, cell cycle protein B binds to CDK1 to form a complex that promotes the cell cycle into M phase [41]. PLK1 is a member of the serine-threonine kinase family, and PLK1 is involved in functions including mitotic entry, centromere segregation and maturation, chromosome alignment, spindle checkpoint signaling, and cytokinesis, it is an essential kinase for DNA damage checkpoints in G2/M phase [42–44]. PLK1 expression levels peak in G2 and M phases and are highly expressed in cells with active proliferation, such as cancer cells. PLK1 phosphorylates CDC25C at multiple sites and promotes its nuclear translocation to increase its activity. Upon activation of CDC25C, it activates the cell cycle protein B-CDK1 complex through dephosphorylation and translocates the complex into the nucleus to promote G2/M progression [45, 46]. Heat shock protein 90β (HSP90β, HSP90AB1) is one of the major isoforms of HSP90 involved in embryonic development, signaling and cellular adaptation [47]. HSP90AB1 was significantly correlated with disease-free survival and overall survival in NSCLC patients, with higher HSP90AB1 levels indicating a poorer prognosis, and lowering HSP90AB1 levels reduced the growth rate of lung cancer cells, causing the cells to remain in the G0/G1 phase [48]. Therefore, cell cycle progression was blocked by inhibiting PLK1, CDK1, and HSP90AB1, which led to the inhibition of cancer cell growth.

As shown by the network pharmacology results, PLK1, CDK1, and HSP90AB1 are the key targets of BSS-MD for the treatment of lung cancer, while PLK1, CDK1, and HSP90AB1 can inhibit the growth of cancer cells by altering the cell-cycle pathway, and at the same time, the results of the molecular docking showed that these targets have good docking activity with the key active ingredients of BSS-MD (Table 4). Therefore, we speculated that BSS-MD might block cell cycle progression by inhibiting the expression of PLK1, CDK1, and HSP90AB1 mRNA and proteins to treat NSCLC. Therefore, we performed in vitro cellular experiments. First, we performed CCK-8 assay and determined that BSS-MD inhibited LEWIS cell viability and promoted apoptosis with a dose correlation (Figure 5A/B/C). Therefore, we further performed qPCR assay, immunofluorescence and protein blotting experiments, and the expression of PLK1, HSP90AB1, CDK1 mRNA, and protein was reduced in the treatment group compared with the control group and the control group ($P < 0.01$) (Figure 6A/B/C), so we concluded that the BSS-MD inhibited the proliferation of NSCLC by regulating the cell cycle. However, this study still has the following shortcomings: (1) Due to the limitations of network pharmacology, this experiment only did a qualitative analysis of the active ingredients of BSS-MD, ignoring the effect of the content of the ingredients on the efficacy of the drug; (2) Only some of the results of network pharmacology were analyzed, and the experimental method was single, the sample size was small, and the experiment was not carried out from various aspects and multiple levels; (3) Only the in vitro cellular experiments were carried out, and in vivo experiments were not carried out to further validate the results.

Conclusion

In summary, in this study, 25 key active ingredients in BSS-MD were initially screened for their effects on 423 targets in NSCLC using network pharmacology and molecular docking technology, which involved PI3K-Akt signaling pathway, MAPK signaling pathway, Ras signaling pathway, Cell cycle, and other signaling pathways. The molecular docking showed that the core components and some of the core targets showed good docking activity, reflecting the therapeutic characteristics of TCM of “multi-targets, multi-pathways and multi-components”. In vitro, experiments further demonstrated that BSS-MD can block cell cycle progression by inhibiting the expression of PLK1, CDK1, and HSP90AB1 mRNAs and proteins to inhibit lung cancer cell growth and promote apoptosis, and emphasized that BSS-MD are promising adjuvants for NSCLC treatment.

References

1. Cao W, Chen HD, Yu YW, et al. Changing profiles of cancer burden worldwide and in China: a secondary analysis of the global cancer statistics 2020. *Chin Med J (Engl)* 2021;134(7):783–791. Available at: http://doi.org/10.1097/CM9.0000000000001474
2. Chen P, Liu Y, Wen Y, Zhou C. Non-small cell lung cancer in China. *Cancer Commun* 2022;42(10):937–970. Available at: http://doi.org/10.1002/cac2.12359
3. Siegel RL, Miller KD, Wagle NS, Jemal A. Cancer statistics, 2023. *CA Cancer J Clin* 2023;73(1):17–48. Available at: http://doi.org/10.3322/caac.21763
4. Ye L, Jia Y, Ji K, et al. Traditional Chinese medicine in the prevention and treatment of cancer and cancer metastasis. *Oncol Lett* 2015;10(3):1240–1250. Available at: http://doi.org/10.3892/ol.2015.3459
5. Zheng Y, Yang S, Si J, et al. Shashen-Maidong Decoction inhibited cancer growth under intermittent hypoxia conditions by suppressing oxidative stress and inflammation. *J Ethnopharmacol* 2022;299:115654. Available at: http://doi.org/10.1016/j.jep.2022.115654
6. He M, Luo Y, Chen L, et al. Shashen maidong decoction: the effect of TNF-α and IL-6 on lung cancer cachexia based on cancer toxicity theory. *Am J Transl Res* 2021;13(6):6752–6758. Available at: https://www.ncbi.nlm.nih.gov/pmc/articles/PMC8290732/
7. Hopkins AL. Network pharmacology: the next paradigm in drug discovery. *Nat Chem Biol* 2008;4(11):682–690. Available at: http://doi.org/10.1038/nchembio.118
8. Sharpee TO, Destexhe A, Kawato M, et al. 25th Annual Computational Neuroscience Meeting: CNS-2016. *BMC Neurosci* 2016;17Suppl1(Suppl1):54. Available at: https://doi.org/10.1186/s12868-016-0283-6
9. Meng XY, Zhang HX, Mezei M, Cui M. Molecular Docking: A Powerful Approach for Structure-Based Drug Discovery. *CAD* 2011;7(2):146–157. Available at: http://doi.org/10.2174/157340911795677602
10. Ru J, Li P, Wang J, et al. TCMSP: a database of systems pharmacology for drug discovery from herbal medicines. *J Cheminform* 2014;6:13. Available at: http://doi.org/10.1186/1758-2946-6-13
11. Liu Z, Guo F, Wang Y, et al. BATMAN-TCM: a Bioinformatics Analysis Tool for Molecular mechANism of Traditional Chinese Medicine. *Sci Rep* 2016;6:21146. Available at: http://doi.org/10.1038/srep21146
12. Bade BC, Dela Cruz CS. Lung Cancer 2020. *Clin Chest Med* 2020;41(1):1–24. Available at: http://doi.org/10.1016/j.ccm.2019.10.001
13. Su XL, Wang JW, Che H, et al. Clinical application and mechanism of traditional Chinese medicine in treatment of lung cancer. *Chin Med J (Engl)* 2020;133(24):2987–2997. Available at: http://doi.org/10.1097/CM9.0000000000001141
14. Li Z, Feiyue Z, Gaofeng L. Traditional Chinese medicine and lung cancer——From theory to practice. *Biomedicine Pharmacotherapy* 2021;137:111381. Available at: http://doi.org/10.1016/j.biopha.2021.111381
15. Yuan L, Zhang PT, Yang ZY. [Study on qi deficiency syndrome distribution and quality of life in patients with advanced non-small cell lung cancer]. *Chinese Journal of Integrated Traditional and Western Medicine* 2011;31(7):880–883. (Chinese) Available at: https://pubmed.ncbi.nlm.nih.gov/21866653/
16. Zheng Y, Yang S, Si J, et al. Shashen-Maidong Decoction inhibited cancer growth under intermittent hypoxia conditions by suppressing oxidative stress and inflammation. *J Ethnopharmacol* 2022;299:115654. Available at:

http://doi.org/10.1016/j.jep.2022.115654
17. Yang Y, Zhou Y. Shashen-Maidong Decoction-Mediated IFN-γ and IL-4 on the Regulation of Th1/Th2 Imbalance in RP Rats. *Biomed Res Int* 2019;2019:6012473. Available at: http://doi.org/10.1155/2019/6012473
18. Zeng P, Li J, Chen Y, Zhang L. The structures and biological functions of polysaccharides from traditional Chinese herbs. *Prog Mol Biol Transl Sci* 2019;2019:423–444. Available at: http://doi.org/10.1016/bs.pmbts.2019.03.003
19. Zhang X, Wang J, Zhu L, et al. Advances in Stigmasterol on its anti-tumor effect and mechanism of action. *Front Oncol* 2022;12:1101289. Available at: http://doi.org/10.3389/fonc.2022.1101289
20. Chang JH, Lai SL, Chen WS, et al. Quercetin suppresses the metastatic ability of lung cancer through inhibiting Snail-dependent Akt activation and Snail-independent ADAM9 expression pathways. *Biochim Biophys Acta Mol Cell Res* 2017;1864(10):1746–1758. Available at: http://doi.org/10.1016/j.bbamcr.2017.06.017
21. Wang Y, Chen M, Yu H, et al. The Role and Mechanisms of Action of Natural Compounds in the Prevention and Treatment of Cancer and Cancer Metastasis. *Front Biosci (Landmark Ed)* 2022;27(6):192. Available at: http://doi.org/10.31083/j.fbl2706192
22. Kanapathipillai M. Treating p53 Mutant Aggregation-Associated Cancer. *Cancers* 2018;10(6):154. Available at: http://doi.org/10.3390/cancers10060154
23. Bao X, Zhang Y, Zhang H, Xia L. Molecular Mechanism of β-Sitosterol and its Derivatives in Tumor Progression. *Front Oncol* 2022;12:926975. Available at: http://doi.org/10.3389/fonc.2022.926975
24. Lin X, Zhang J, Chen L, et al. Tyrosine phosphorylation of Rab7 by Src kinase. *Cell Signal* 2017;35:84–94. Available at: http://doi.org/10.1016/j.cellsig.2017.03.006
25. Noorolyai S, Shajari N, Baghbani E, et al. The relation between PI3K/AKT signalling pathway and cancer. *Gene* 2019;698:120–128. Available at: http://doi.org/10.1016/j.gene.2019.02.076
26. Li S, Li H, Cao Y, et al. Integrated bioinformatics analysis reveals CDK_1 and PLK_1 as potential therapeutic targets of lung adenocarcinoma. *Medicine (Baltimore)* 2021;100(32):e26474. Available at: http://doi.org/10.1097/MD.0000000000026474
27. Iksen, Pothongsrisit S, Pongrakhananon V. Targeting the PI3K/AKT/mTOR Signaling Pathway in Lung Cancer: An Update Regarding Potential Drugs and Natural Products. *Molecules* 2021;26(13):4100. Available at: http://doi.org/10.3390/molecules26134100
28. Guo Y, Pan W, Liu S, et al. ERK/MAPK signalling pathway and tumorigenesis. *Exp Ther Med* 2020;19(3):1997–2007. Available at: http://doi.org/10.3892/etm.2020.8454
29. Jiang M, Zhou L, Xu N, An Q. Hydroxysafflor yellow A inhibited lipopolysaccharide-induced non-small cell lung cancer cell proliferation, migration, and invasion by suppressing the PI3K/AKT/mTOR and ERK/MAPK signaling pathways. *Thoracic Cancer* 2019;10(6):1319–1333. Available at: http://doi.org/10.1111/1759-7714.13019
30. Rauen KA. The RASopathies. *Annu Rev Genom Hum Genet* 2013;14(1):355–369. Available at: http://doi.org/10.1146/annurev-genom-091212-153523
31. Cuesta C, Arévalo-Alameda C, Castellano E. The Importance of Being PI3K in the RAS Signaling Network. *Genes* 2021;12(7):1094. Available at: http://doi.org/10.3390/genes12071094
32. Tang SM, Deng XT, Zhou J, et al. Pharmacological basis and new insights of quercetin action in respect to its anti-cancer effects. *Biomed Pharmacother* 2020;121:109604. Available at: http://doi.org/10.1016/j.biopha.2019.109604
33. Lim S, Kaldis P. Cdks, cyclins and CKIs: roles beyond cell cycle regulation. *Development* 2013;140(15):3079–3093. Available at: http://doi.org/10.1242/dev.091744
34. Michowski W, Chick JM, Chu C, et al. Cdk_1 Controls Global Epigenetic Landscape in Embryonic Stem Cells. *Molecular Cell* 2020;78(3):459–476.e13. Available at: http://doi.org/10.1016/j.molcel.2020.03.010
35. Odle RI, Florey O, Ktistakis NT, Cook SJ. CDK_1, the Other 'Master Regulator' of Autophagy. *Trends Cell Biol* 2021;31(2):95–107. Available at: http://doi.org/10.1016/j.tcb.2020.11.001
36. Gregg T, Sdao SM, Dhillon RS, et al. Obesity-dependent CDK_1 signaling stimulates mitochondrial respiration at complex I in pancreatic β-cells. *J Biol Chem* 2019;294(12):4656–4666. Available at: http://doi.org/10.1074/jbc.RA118.006085
37. Brown NR, Korolchuk S, Martin MP, et al. CDK_1 structures reveal conserved and unique features of the essential cell cycle CDK. *Nat Commun* 2015;6:6769. Available at: http://doi.org/10.1038/ncomms7769
38. Faienza F, Polverino F, Rajendraprasad G, et al. $AMBRA_1$ phosphorylation by CDK_1 and PLK_1 regulates mitotic spindle orientation. *Cell Mol Life Sci* 2023;80(9):251. Available at: http://doi.org/10.1007/s00018-023-04878-6
39. Lindqvist A, Rodríguez-Bravo V, Medema RH. The decision to enter mitosis: feedback and redundancy in the mitotic entry network. *J Cell Biol* 2009;185(2):193–202. Available at: http://doi.org/10.1083/jcb.200812045
40. Hégarat N, Rata S, Hochegger H. Bistability of mitotic entry and exit switches during open mitosis in mammalian cells. *Bioessays* 2016;38(7):627–643. Available at: http://doi.org/10.1002/bies.201600057
41. Hnit SST, Yao M, Xie C, et al. Transcriptional regulation of G2/M regulatory proteins and perturbation of G2/M Cell cycle transition by a traditional Chinese medicine recipe. *J Ethnopharmacol* 2020;251:112526. Available at: http://doi.org/10.1016/j.jep.2019.112526
42. Combes G, Alharbi I, Braga LG, Elowe S. Playing polo during mitosis: PLK1 takes the lead. *Oncogene* 2017;36(34):4819–4827. Available at: http://doi.org/10.1038/onc.2017.113
43. Saurin AT. Kinase and Phosphatase Cross-Talk at the Kinetochore. *Front Cell Dev Biol* 2018;6:62. Available at: http://doi.org/10.3389/fcell.2018.00062
44. Porter LA, Donoghue DJ. Cyclin B_1 and CDK_1: nuclear localization and upstream regulators. *Prog Cell Cycle Res* 2003;5:335–347. Available at: https://pubmed.ncbi.nlm.nih.gov/14593728/
45. Liu K, Zheng M, Lu R, et al. The role of CDC25C in cell cycle regulation and clinical cancer therapy: a systematic review. *Cancer Cell Int* 2020;20:213. Available at: http://doi.org/10.1186/s12935-020-01304-w
46. Li J, Huang HY, Lin YCD, et al. Cinnamomi ramulus inhibits cancer cells growth by inducing G2/M arrest. *Front Pharmacol* 2023;14:1121799. Available at: http://doi.org/10.3389/fphar.2023.1121799
47. Rong BX, Jiang XL, Yang SY, et al. Upregulation of Hsp90-beta and annexin A_1 correlates with poor survival and lymphatic metastasis in lung cancer patients. *J Exp Clin Cancer Res* 2012;31(1):70. Available at: http://doi.org/10.1186/1756-9966-31-70
48. Wang X, Wang Y, Feng L, et al. Elevated expression of lung development-related protein HSP90β indicates poor prognosis in non-small cell lung cancer through affecting the cell cycle and apoptosis. *Sig Transduct Target Ther* 2021;6(1):82. Available at: http://doi.org/10.1038/s41392-021-00465-y